Spinal muscular atrophy patient iPSC-derived motor neurons have reduced expression of proteins important in neuronal development

Heidi R. Fuller[1, 2], Berhan Mandefro[3, 4], Sally L. Shirran[5], Andrew R. Gross[3], Anjoscha S. Kaus[3], Catherine H. Botting[5], Glenn E. Morris[1, 2], Dhruv Sareen[3, 4, 6*]

[1]Institute for Science and Technology in Medicine, Keele University, United Kingdom, [2]Wolfson Centre for Inherited Neuromuscular Disease, RJAH Orthopaedic Hospital, United Kingdom, [3]Cedars-Sinai Medical Center, Board of Governors-Regenerative Medicine Institute, USA, [4]iPSC Core, USA, [5]BSRC Mass Spectrometry and Proteomics Facility, University of St Andrews, United Kingdom, [6]Cedars-Sinai Medical Center, Department of Biomedical Sciences, USA

Submitted to Journal:
Frontiers in Cellular Neuroscience

Article type:
Original Research Article

Manuscript ID:
170378

Received on:
30 Sep 2015

Revised on:
03 Dec 2015

Frontiers website link:
www.frontiersin.org

Conflict of interest statement

The authors declare that the research was conducted in the absence of any commercial or financial relationships that could be construed as a potential conflict of interest

Author contribution statement

HRF participated in the study design, conducted experiments, analyzed data, and wrote the manuscript. SS and CB conducted the mass spectrometry analysis. BM performed differentiation and culturing of the iPS cells. ARG performed the qRT-PCR experiments. AK performed the gemin2 quantitative western blotting. GEM participated in the study design and provided reagents for the study. DS wrote manuscript, participated in the study design, conducted iPS cell characterization, neuronal differentiation experiments and analyzed data. The manuscript was written through contributions of all authors. All authors have given approval to the final version of the manuscript.

Keywords

SMA, spinal muscular atrophy, ubiquitin-like modifier activating enzyme 1, uba1, Uchl1, Ubiquitin carboxyl-terminal esterase L1, Proteomics, Induced Pluripotent Stem Cells, IPSC, motor neuron

Abstract

Word count: 206

Spinal muscular atrophy (SMA) is an inherited neuromuscular disease primarily characterized by degeneration of spinal motor neurons, and caused by reduced levels of the SMN protein. Previous studies to understand the proteomic consequences of reduced SMN have mostly utilized patient fibroblasts and animal models. We have derived human motor neurons from type I SMA and healthy controls by creating their induced pluripotent stem cells (iPSCs). Quantitative mass spectrometry of these cells revealed increased expression of 63 proteins in control motor neurons compared to respective fibroblasts, whereas 30 proteins were increased in SMA motor neurons versus their fibroblasts. Notably, UBA1 was significantly decreased in SMA motor neurons, supporting evidence for ubiquitin pathway defects. Subcellular distribution of UBA1 was predominantly cytoplasmic in SMA motor neurons in contrast to nuclear in control motor neurons; suggestive of neurodevelopmental abnormalities. Many of the proteins that were decreased in SMA motor neurons, including beta III-tubulin and UCHL1, were associated with neurodevelopment and differentiation. These neuron-specific consequences of SMN depletion were not evident in fibroblasts, highlighting the importance of iPSC technology. The proteomic profiles identified here provide a useful resource to explore the molecular consequences of reduced SMN in motor neurons, and for the identification of novel biomarker and therapeutic targets for SMA.

Funding statement

This work was supported by The RJAH Institute of Orthopaedics, UK (H.F.), The SMA Trust, UK (H.F.), Cedars-Sinai Institutional startup funds (D.S), California Institute for Regenerative Medicine Grant RT-02040 (D.S.), National Center for Advancing Translational Sciences (NCATS), Grant UL1TR000124 (D.S.), and the Wellcome Trust [grant number 094476/Z/10/Z] which funded the purchase of the TripleTOF 5600 mass spectrometer at the BSRC Mass Spectrometry and Proteomics Facility, University of St Andrews (S.S. and C.B.). D.S. is also supported by funds from National Institute of Health (NINDS) grant U54NS091046. The funders had no role in study design, data collection and analysis, decision to publish, or preparation of the manuscript.

Ethics statement

(Authors are required to state the ethical considerations of their study in the manuscript including for cases where the study was exempt from ethical approval procedures.)

Did the study presented in the manuscript involve human or animal subjects: No

Spinal muscular atrophy patient iPSC-derived motor neurons have reduced expression of proteins important in neuronal development

Heidi R. Fuller[1,2], Berhan Mandefro[3,4], Sally L. Shirran[6], Andrew R. Gross[3†], Anjoscha Kaus[3†], Catherine H. Botting[6], Glenn E. Morris[1,2], Dhruv Sareen[3,4,5].*

[1]Wolfson Centre for Inherited Neuromuscular Disease, RJAH Orthopaedic Hospital, Oswestry, SY10 7AG, UK, [2]Institute for Science and Technology in Medicine, Keele University, Staffordshire, ST5 5BG, UK, [3]Board of Governors-Regenerative Medicine Institute, Cedars-Sinai Medical Center, Los Angeles, CA, 90048; [4]iPSC Core, The David and Janet Polak Foundation Stem Cell Core Laboratory; [5]Department of Biomedical Sciences, Cedars-Sinai Medical Center, Los Angeles, CA 90048, USA. [6]BSRC Mass Spectrometry and Proteomics Facility, University of St Andrews, North Haugh, Fife, KY16 9ST, UK.

†These authors contributed equally.

*Corresponding Author.
Board of Governors-Regenerative Medicine Institute, Cedars-Sinai Medical Center, Los Angeles, CA, 90048; email: Dhruv.Sareen@cshs.org

Keywords

SMA, spinal muscular atrophy, ubiquitin-like modifier activating enzyme 1, UBA1, UCHL1, ubiquitin carboxyl-terminal esterase L1, proteomics, induced pluripotent stem cells, iPSC, motor neuron.

Abstract

Spinal muscular atrophy (SMA) is an inherited neuromuscular disease primarily characterized by degeneration of spinal motor neurons, and caused by reduced levels of the SMN protein. Previous studies to understand the proteomic consequences of reduced SMN have mostly utilized patient fibroblasts and animal models. We have derived human motor neurons from type I SMA and healthy controls by creating their induced pluripotent stem cells (iPSCs). Quantitative mass spectrometry of these cells revealed increased expression of 63 proteins in control motor neurons compared to respective fibroblasts, whereas 30 proteins were increased in SMA motor neurons versus their fibroblasts. Notably, UBA1 was significantly decreased in SMA motor neurons, supporting evidence for ubiquitin pathway defects. Subcellular distribution of UBA1 was predominantly cytoplasmic in SMA motor neurons in contrast to nuclear in control motor neurons; suggestive of neurodevelopmental abnormalities. Many of the proteins that were decreased in SMA motor neurons, including beta III-tubulin and UCHL1, were associated with neurodevelopment and differentiation. These neuron-specific consequences of SMN depletion were not evident in fibroblasts, highlighting the importance of iPSC technology. The proteomic profiles identified here provide a useful resource to explore the molecular consequences of reduced SMN in motor neurons, and for the identification of novel biomarker and therapeutic targets for SMA.

1. Introduction

Spinal Muscular Atrophy (SMA) is a recessively inherited neuromuscular disease displaying a wide range of severity, from the most severe Type I (diagnosed somewhere between birth to 6 months of age), to adult onset, Type IV. SMA is primarily characterized by loss of function and degeneration of lower motor neurons in the anterior horn of the spinal cord, and is caused by reduced levels of the survival of motor neurons (SMN) protein, which is encoded by two genes, *SMN1* and *SMN2*[1]. Most of the mRNA transcribed from the *SMN2* gene is alternatively spliced to omit exon 7 and any protein translated from such "delta7" mRNA is unstable and rapidly degraded[1,2,3]. In SMA patients, the *SMN1* gene is mutated or deleted and only a small amount of stable and functional SMN is produced from the *SMN2* gene, with the more severe phenotypes having the least SMN[4,5].

SMN is a ubiquitously-expressed protein that plays a central role RNA biogenesis; regulating the assembly of small nuclear ribonucleic proteins (snRNPs) in the cytoplasm and their subsequent transport into the nucleus[1,6]. Aside from this housekeeping role, SMN also appears to have a neuronal-specific role in mRNA processing, where it interacts with hnRNP-R to transport β-actin mRNA in axons[7,8]. Despite this knowledge about the cellular functions of SMN, it has become clear, from studies with mouse models, that defects in RNA splicing or axonal transport do not fully explain why lower motor neurons are particularly vulnerable to reduced levels of SMN[9, 10, 11, 12, 13].

Previous attempts to understand the molecular consequences of reduced SMN expression in SMA have largely been focused on patient fibroblasts and animal models. Various animal models of SMA are available[14], but their intrinsic differences from humans may prevent effective translation to clinical trials. In addition, animal models of SMA may not be as amenable to high-throughput drug discovery programs, compared to patient cells. SMA patient skin fibroblasts are easily accessible and can be expanded in culture, in large quantities, with relative ease. Although SMA patient skin fibroblasts display reduced SMN levels in culture, the skin itself is pathophysiologically spared in patients, suggesting that these cells respond differently to, or have different requirements for, SMN, compared with lower motor neurons.

Reprogramming somatic cell types to pluripotency by human induced pluripotent stem cell (iPSC) technology preserves the patient's genome and its errors and allows investigators to observe these diseased genotypes within any human cell type[15,16]. Human iPSCs can provide an unlimited supply of patient cells (for example, lower motor neurons for SMA), which can then be studied *in vitro*. We have previously shown that iPSCs from type I SMA patients are capable of differentiating into motor neurons that lack *SMN1* expression and demonstrate selective motor neuron death over time[17,18,19]. Whilst targeted biochemical studies enable the characterization of known protein pathways in such cellular models, large-scale quantitative mass spectrometry approaches offer the possibility of studying the proteome in an unbiased fashion, and can be useful for assessing the suitability of cellular models[20].

The aim of this study was to conduct the first comprehensive evaluation of the proteome of SMA patient iPSC-derived motor neurons and provide a comparison against genetically matched fibroblasts using quantitative mass spectrometry (i.e. iTRAQ). We were particularly interested to

139 examine whether there are down-stream effects of reduced SMN in iPSC-derived motor neuron
140 cultures, not found in fibroblasts, as these could be useful for exploring the particular
141 vulnerability of motor neurons in SMA. In a 4-plex quantitative proteomics comparison
142 (iTRAQ), we compared the proteome of SMA and control motor neurons with the fibroblast cell
143 lines from which they were originally derived. We provide evidence that motor neurons from
144 SMA patients display reduced expression of proteins involved in developmental and
145 differentiation pathways, including ubiquitin-activating enzyme 1 (UBA1) and ubiquitin
146 carboxyl-terminal esterase L1 (UCHL1), and that most of these changes are distinct from those
147 seen in the fibroblast cell lines from which the iPSCs were derived.
148
149
150 **2. Methods**
151
152
153 ***2.1 Ethics Statement***
154
155 Human dermal fibroblasts or lymphoblastoid cell lines (LCLs) were obtained from the Coriell
156 Institute for Medical Research. The Coriell Cell Repository maintains the consent and privacy of
157 the donor LCLs. All the cell lines and protocols in the present study were carried out in
158 accordance with the guidelines approved by Stem Cell Research Oversight committee (SCRO)
159 and Institutional Review Board (IRB) at the Cedars-Sinai Medical Center under the auspice IRB-
160 SCRO Protocols Pro00032834 (iPSC Core Repository and Stem Cell Program), Pro00024839
161 (Using iPS cells to develop novel tools for the treatment of Spinal Muscular Atrophy) and
162 Pro00036896 (Sareen Stem Cell Program).
163
164
165 ***2.2 Generation of human iPSCs using episomal plasmids***
166
167 Human iPSCs were generated as described previously[18, 19, 21, 22]. Briefly, iPS cell lines were
168 reprogrammed from dermal fibroblasts into virus-free iPSC lines with the Nucleofector Kit using
169 1.5 µg of each episomal plasmid (Addgene) expressing 6 factors: OCT4, SOX2, KLF4, L-MYC,
170 LIN28, and p53 shRNA (pCXLE-hOCT3/4-shp53-F, pCXLE-hUL, and pCXLE-hSK). This
171 method has a significant advantage over viral transduction because exogenously introduced
172 genes do not integrate and are instead expressed episomally in a transient fashion. Dermal
173 fibroblasts (1 x 10^6 cells per nucleofection) were harvested, centrifuged at 1500 rpm for 5 min,
174 re-suspended carefully in Nucleofector® Solution and the U-023 program was applied. These
175 nucleofected cells were plated on feeder-independent BD Matrigel™ growth factor-reduced
176 Matrix (Corning/BD Biosciences, #354230). All cultures were maintained at 20% O2 during the
177 reprogramming process. Individual iPSC colonies with ES/iPSC-like morphology appeared
178 between day 25-32 and those with best morphology were mechanically isolated, transferred onto
179 12-well plates with fresh Matrigel™ Matrix, and maintained in mTeSR®1 medium. The iPSC
180 clones were further expanded and scaled up for further analysis.
181
182
183 ***2.3 Karyotype***
184

The SMA and control iPS cell lines were incubated in Colcemid (100 ng/mL; Life Technologies) for 30 min at 37°C and then dissociated using trypsin (TrypLE) for 10 min. They were then washed in phosphate buffered saline (PBS) and incubated at 37°C in 5 mL of hypotonic solution (1g potassium chloride (KCl), 1g sodium citrate in 400 mL water) for 30 min. The cells were centrifuged for 2.5 min at 1500 RPM and resuspended in fixative (methanol: acetic acid, 3:1) at room temperature for 5 min. This was repeated twice, and finally cells were resuspended in 500 µL of fixative solution and submitted to the Cedars-Sinai Clinical Cytogenetics Core for G-Band karyotyping.

2.4 PluriTest

High quality total RNA was isolated from undifferentiated iPSCs, H9 hESCs, fibroblasts and primary human neural progenitors using the RNeasy Mini Kit (Qiagen) and subsequently run on a Human HT-12 v4 Expression BeadChip Kit (Illumina). The raw data file (idat file) was subsequently uploaded on to an open-source and easily accessible Pluritest widget online (www.pluritest.org). PluriTest is a transciptomics and bioinformatics based characterization test for determining pluripotency of a reprogrammed cell line[23]. In this test mRNA expression values of all probes including pluripotency-associated genes are scored against samples in the stem cell model matrix, consisting of 264 pluripotent cell lines (223 hESC and 41 human iPSC) and 204 samples derived from somatic cells and tissues. The red and blue background hint to the empirical distribution of the pluripotent (red) and non-pluripotent samples (blue) in the Müller et al.[23] test data set. An iPSC line is considered a bona-fide fully reprogrammed pluripotent cell line when the pluripotency score is above 20 and the novelty score is below 1.6. A typical chart combines pluripotency score on y-axis and novelty score on x-axis.

2.5 Neural and motor neuron differentiation

The SMA patient and control subject iPSCs were grown until approximately 90% confluent as colonies under normal maintenance conditions before the start of the differentiation. The single cell iPSCs were gently lifted by accutase treatment for 5 min at 37°C. Subsequently, 1.5-2.5 X 10^4 cells were placed in each well of a 384 well plate in defined neuroectodermal differentiation medium (NDM) composed of Iscove's modified Dulbecco's medium supplemented with B27–vitamin A (2%) and N2 (1%), with the addition of 0.2 µM LDN193189 and 10 M SB431542 (NDM+LS). This is a modified dual-SMAD protocol[24]. All days of differentiation described are post-iPSC (PI) stage (day 0). At day 2 PI, neural aggregates were transferred to low adherence polyhydroxyethylmethacrylate (poly-HEMA) coated flasks and cultured in suspension. After this point, the differentiation protocol was optimized to reliably generate lower spinal motor neurons. At 5 days PI, neuroectodermal aggregates were seeded on laminin-coated (50 µg/mL; Sigma #L2020) six well plates to induce neural rosette formation. From days 12-19 PI, the media was changed to motor neuron specification media (MNSM) supplemented with 0.25 µM all-trans retinoic acid (ATRA), 1 µM purmorphamine, 20 ng/mL brain-derived neurotrophic factor (BDNF), 20 ng/mL glial cell line–derived neurotrophic factor (GDNF), 200 ng/mL ascorbic acid, and 1 µM dibutyryl cyclic adenosine monophosphate (db-cAMP). Between days 17-19 PI, neural rosettes were selected using rosette selection media (StemCell Technologies, #05832).

231 The isolated rosettes were subsequently cultured in motor neuron precursor expansion media
232 (MNPEM) consisting of NDM, 0.1 µM ATRA, 1 µM purmorphamine, 100 ng/mL EGF and 100
233 ng/mL FGF2. These iPSC-derived motor neuron precursor spheres (iMPS) can be expanded
234 over a 2-7 week period by an automated chopping method[25]. The iMPS were differentiated
235 further for 21-28 days, for maturation into into motor neurons before harvesting or fixation.
236 These motor neuron samples were used in iTRAQ and other experiments described here. Briefly,
237 iMPS were dissociated with accutase and then seeded onto laminin-coated plates (5-8 X 10^5
238 cells/cm^2) in MN maturation media (MNMM) stage 1 for 7 days consisting of NDM,
239 supplemented with 0.1 µM ATRA, 1 µM purmorphamine, 10 ng/mL BDNF, 10 ng/mL GDNF,
240 200 ng/mL ascorbic acid, 1 µM db-cAMP, and 2.5 µM *N*-[(3,5-Difluorophenyl)acetyl]-L-alanyl-
241 2-phenyl]glycine-1,1-dimethylethyl ester (DAPT; inhibitor of γ-secretase; Cayman Chemicals,
242 #13197). The remainder of terminal differentiation was carried out in Neurobasal supplemented
243 with 1% NEAA, 0.5% GlutaMax, 1% N2, 10 ng/mL BDNF, 10 ng/mL GDNF, 200 ng/mL
244 ascorbic acid, 1 µM db-cAMP, and 0.1 µM.
245
246
247 ***2.6 Quantitative proteomics comparison***
248
249 Cell pellets (containing approximately 6 x 10^4 cells) were extracted in 4 volumes of extraction
250 buffer (w/v) containing 6M Urea, 2M Thiourea, 2% CHAPS and 0.5% SDS in HPLC-grade
251 water (Sigma Chromasolv plus). The extracts were sonicated briefly and left on ice for 10 min,
252 followed by centrifugation at 13,000 x g for 10 min at 4°C to pellet any insoluble material. The
253 proteins were precipitated in 6 volumes of ice cold acetone overnight at -20°C. The acetone
254 precipitates were pelleted by centrifugation at 13,000 x g for 10 min at 4°C and the supernatant
255 was carefully removed and discarded. The pellets were allowed to air-dry, and were then
256 resuspended in 500 mM tetraethylammonium bromide (TEAB). The protein concentration in
257 each group was determined using a Bradford assay.
258
259
260 ***2.7 Sample preparation for mass spectrometry analysis***
261
262 Reduction, alkylation and digestion steps were performed according to the recommendations
263 detailed in the iTRAQ labelling kit (AB Sciex). The extracts were digested with trypsin (5µg per
264 100µg of protein) overnight at 37°C, followed by reduction and alkylation steps performed
265 according to instructions outlined in the iTRAQ labelling kit. The digests were subsequently
266 dried down in a vacuum centrifuge and iTRAQ labelling was carried out according to the
267 instructions in the iTRAQ labelling kit. The iTRAQ tags were assigned to samples as follows:
268 114- fibroblasts from control GMO3814 (n=1); 115- motor neurons – derived from control
269 GMO3814 (n=1); 116- fibroblasts from Type 1 SMA patient GMO0232 (n=1); 117- motor
270 neurons – derived from Type 1 SMA patient GMO0232 (n=1). Each tag was incubated with 60
271 µg of total protein (as determined by a Bradford protein assay).
272
273
274 ***2.8 Mass spectrometry analysis***
275

The combined 4-plex iTRAQ labelled peptides were concentrated in a vacuum concentrator and resuspended in 0.6 mL of loading Buffer A_{scx} (10 mM monopotassium phosphate (KH_2PO_4), 20% acetonitrile (MeCN), pH 3.0), followed by sonication. The pH was adjusted to 3.0 with 0.5 M orthophosphoric acid (H_3PO_4). The peptides were then separated by strong cation exchange chromatography as described previously[26].

Each SCX fraction was analysed by nanoLC ESI MSMS using a TripleTOF 5600 tandem mass spectrometer (ABSciex, Foster City, CA) as described previously[26]. The raw mass spectrometry data file was subsequently analysed using ProteinPilot 4.5 software with the Paragon™ and ProGroup™ algorithms (ABSciex) against the human sequences in the Swiss-Prot database (http://www.uniprot.org/, accessed in July 2013; containing 539,616 sequences in total and 20,255 human sequences). Searches were performed using the preset iTRAQ settings in ProteinPilot. Trypsin was selected as the cleavage enzyme and MMTS modification of cysteines with a 'Thorough ID' search effort. ProteinPilot's Bias correction, which assumes that most proteins do not change in expression and corrects for unequal mixing during the combining of labelled samples, was applied, with ratios of 1.0234 for the 115:114 labels, 0.6653 for 116:114 and 1.2362 for 117:114. Finally, detected proteins were reported with a Protein Threshold (Unused ProtScore (confidence)) >0.05 and used in the quantitative analysis if they were identified with three or more peptides with 95% confidence or above. P-values for the iTRAQ ratios were calculated by the ProteinPilot software. A False Discovery Rate (FDR) analysis was also performed against a concatenated database of forward and reverse protein sequences as a decoy database, using the Proteomics System Performance Evaluation Pipeline (PSPEP) in ProteinPilot, which reported 2093 proteins above a 5% local (for a given peptide) false discovery rate threshold and 2217 proteins above a 1% global false discovery rate threshold.

2.9 Immunohisto/cytochemistry

Human iPS cell lines and their differentiated cell types were plated on glass coverslips in optical-bottom 96-well plates (Thermo, # 165305) and subsequently fixed in 4% paraformaldehyde (Figure 1) or acetone/methanol (all other Figures). For Figure 1: cells were blocked in 5% normal donkey serum with 0.1% Triton X-100 and incubated with primary antibodies (Supplementary File S1) either for either 1 hour at room temperature or overnight at 4°C. Cells were then rinsed and incubated in species-specific AF488, AF594 or AF647-conjugated secondary antibodies followed by Hoechst 33258 (0.5 µg/mL; Sigma) to counterstain nuclei. Cells were imaged using Molecular Devices Image Express Micro high-content imaging system or using Leica microscopes. For all other Figures: coverslips were incubated in primary antibodies (Supplementary File S1) for 1 hour at room temperature. Cells were then rinsed and incubated for 1 hour with 5 µg mL^{-1} goat anti-mouse ALEXA 488 (Molecular Probes, Eugene, OR) or swine anti-rabbit ALEXA 546, diluted in PBS containing 1% horse serum, 1% fetal bovine serum and 0.1% BSA, followed by addition of DAPI (diamidinophenylindole 200 ng mL-1) for the final 5 min of incubation. After washing, coverslips were mounted on slides in Hydromount (Merck). High magnification images were obtained using a Leica SP5 confocal microscope with a 63×oil immersion objective.

2.10 SDS-polyacrylamide gel electrophoresis and western blotting

Protein extracts from three separate SMA and three control iPSC-derived motor neuron cell lines were prepared by boiling in SDS sample loading buffer (2% SDS, 5% 2-mercaptoethanol, 62.5 mM Tris-HCl, pH 6.8), for 2 min. Proteins were subjected to SDS-PAGE (Biorad) using 12.5% polyacrylamide gels. A horizontal slice was excised from the gel (clear from the molecular weight of proteins of interest) for staining with Coomassie blue as an internal loading control. The proteins on the remaining part of the gel were then transferred to nitrocellulose membranes by western blotting. After blocking non-specific sites with 4% powdered milk solution, membranes were incubated with primary antibodies (Supplementary File S1), and diluted in dilution buffer (PBS, 1% fetal bovine serum, 1% horse serum and 0.1% BSA). Antibody reacting bands were visualized by development with either peroxidase-labeled goat anti-mouse Ig or peroxidise-labeled swine anti-rabbit Ig (1 µg/mL in dilution buffer) and a chemiluminescent detection system (West Pico or West Femto, Pierce), followed by visualization using a Gel Image Documentation system (Biorad). Densitometry measurements of antibody reactive bands were derived using Image J software (v1.46) and were normalized to the densitometry of the Coomassie stained gel, as described by Eaton et al. (2013)[27]. For quantification of the Coomassie gel, a rectangular box was drawn around several bands in each lane for densitometry measurement (the details of the molecular weight range of these bands in each case is provided in each figure). The box was then copied and carefully pasted to the same position for every sample lane. In instances where the image quality of the Coomassie stained gel was low due to low protein levels (i.e. Figure 1d and 4), the contrast was adjusted uniformly across the gel to enhance the signal. Unpaired, heteroscedastic t-tests were conducted (Microsoft Excel) to assess whether differences in densitometry were statistically significant.

2.11 Quantitative RT-PCR

Total RNA was isolated from three separate SMA and three control iPSC-derived motor neuron cell lines using the Quick-RNA MiniPrep kit (Zymo Research). A volume of 2µg of RNA was reverse transcribed using a High Capacity cDNA Reverse Transcription Kit by Applied Biosystems. Reactions were performed in triplicate using SYBR Select Master Mix (Applied Biosystems) using specific primer sequences (Supplementary File S3). Samples were held at 50°C for 2 min, 95°C for 2 min, and then cycled 40 times between 95°C for 15 seconds and 60°C for 30 seconds. A melting curve was recorded from 65°C to 95°C in 0.5^{o}C increments over 0.05 second steps. Expression of target genes was normalized to the expression of RPL13 ribosomal Protein L13A and calculated by the DDCT method[28,29]. Unpaired, one-tailed t-tests were conducted using Graphpad Prism software, to assess the statistical significance of the expression data.

3. Results

3.1 Generation of human induced pluripotent stem cell-derived motor neurons

367 Induced pluripotent stem cells (iPSCs) generated from type I SMA patients and healthy controls
368 (see Supplementary File S2 for origin, clinical history and genetics) were generated as previously
369 described[19]. Positive immunostaining confirmed the presence of nuclear and surface
370 pluripotency antigens, along with normal G-band karyotype (Figure 1a). A gene-chip and
371 bioinformatics based PluriTest[23] characterization of the control and SMA iPS cell lines
372 confirmed pluripotency in all SMA and control iPSC lines (determined by the presence of a
373 PluriTest score of greater than 20 in pluripotency and below 1.6 in novelty) (Figure 1b). The red
374 cloud and surrounding region signifies pluripotent samples, while anything outside the red cloud
375 and in the blue area are non-pluripotent samples, based on well-characterized pluripotent stem
376 cell data set[23]. The SMA and control iPSCs were then directed towards a lower spinal motor
377 neuron fate by following stepwise differentiation paradigm mimicking human spinal cord
378 development. The iPSCs first underwent neuroectodermal specification followed by addition of
379 caudo-ventralizing factors (all-trans retinoic acid and sonic hedgehog agonist, purmorphamine)
380 and maturation. At this point, the motor neurons are electrophysiologically active, as we have
381 demonstrated previously[21]. These motor neuron cultures contained few nestin progenitors and
382 Map2 a/b neurons (dendritic marker) (<10%), pan-neurons marker βIII-tubulin (>60%) with few
383 astroglial (GFAP) cells, and mostly SMI32 and ISL1 (Islet-1) positive motor neurons (~40%).
384 Nkx6.1 and ChAT are spinal motor neuron markers that are expressed in both control and SMA-
385 derived motor neurons (Figure 1c).
386
387
388 ***3.2 SMN depletion has contrasting downstream effects on the proteome of motor neurons***
389 ***compared to genetically matched fibroblasts.***
390
391 To determine the downstream proteomic consequences of reduced SMN in iPSC-derived motor
392 neuron cultures, we conducted a 4-plex quantitative comparison of the proteome of 32i SMA
393 motor neurons with 14i control motor neurons, alongside the fibroblast cell lines from which
394 they were originally derived (i.e. GM00232 and GM03814) using iTRAQ-mass spectrometry.
395 This approach detected (and subsequently quantified) 2,093 proteins, with a 5% local false
396 discovery rate threshold (Supplementary Table 1). Even with the very latest technology,
397 identification of proteins using mass spectrometry is limited to approximately the top 30% of the
398 total proteome[20]. It is possible, therefore, that due to the limitations of the technique, some
399 important changes may not have been detected. For example, neither SMN nor any other known
400 components of the SMN core complex were among the 2,093 proteins that were detected and
401 quantified, presumably because the SMN core complex appears to be a minor component of the
402 entire cellular proteome[30]. Nonetheless, a statistically significant reduction of SMN protein in the
403 SMA motor neurons was verified by western blotting (Figure 1d) and a reduction of full-length
404 SMN gene expression was verified by RT-PCR (Figure 1e). A reduction of the SMN-binding
405 protein, gemin2, was also seen by western blot analysis (Supplementary File S4), and is
406 consistent with previous reports showing reduced levels of SMN complex components in SMA
407 (e.g.[31]).
408
409 For reliable quantification, proteins identified from fewer than three peptides were excluded
410 from the list, followed by exclusion of those with average iTRAQ ratios of less than 1.25 or
411 greater than 0.75, and finally exclusion of those with a p value of >0.05. It is possible that the
412 filtering criteria applied here may have resulted in some genuinely differentially expressed

proteins being omitted from the final analysis, and so we have supplied supplementary tables of raw data to enable researchers to analyse the data differently, or to select other protein targets for further study (Supplementary Table 1 and 2). After applying the filtering criteria, 99 proteins were differentially expressed, with statistical significance, when SMA motor neurons were compared to control motor neurons (bold; Supplementary Table 1a and Figure 2a). The differential expression of several of the 99 proteins can be attributed to presence of some GFAP positive astrocytes, desmin-positive myoblasts in the original fibroblasts and collagen VI positive cells (Supplementary File, S5). Although an equal total protein concentration was loaded onto each iTRAQ tag, it is not yet possible to derive precisely synchronised, homogeneous populations of mature neurons from iPS cells.

When SMA fibroblasts were quantitatively compared to control fibroblasts, 18 proteins were differentially expressed (Supplementary Table 1b; bold font and Figure 2b). Interestingly, only one of these 18 proteins, collagen alpha-3 VI, was also differentially expressed in the same direction when the SMA motor neurons were compared to control motor neurons (p value 0.00004) (Supplementary Table 1 and Figure 2). Six of the 18 proteins were differentially expressed in one direction (i.e. up- or down-regulated) when SMA fibroblasts were compared to control fibroblasts and then expressed in the opposite direction when SMA MNs were compared to control MNs (Table 1, Supplementary Table 1 and Figure 2).

3.3 Dysregulation of developmental and differentiation pathways in SMA motor neurons

A quantitative comparison of protein expression in the control motor neurons compared to their respective genetically matched fibroblast cells revealed that 175 proteins were differentially expressed, whereas just 82 proteins were differentially expressed in the SMA motor neurons when compared to the fibroblasts from which they were derived (Supplementary Table 1c and 1d and Supplementary Table 2a-c). Only 55 of these differentially expressed proteins were common to both the SMA and the control cells; of these, 17 proteins were increased in expression in the motor neurons compared to the fibroblast cells (Supplementary Table 2a-c and Figure 3a).

To gain some insight into the likely functions of the 46 proteins that were increased in expression <u>only</u> in the control motor neurons vs control fibs (and not increased in the SMA motor neurons vs SMA fibs), gene ontology analysis was performed using the the Database for Annotation, Visualization and Integrated Discovery (DAVID)[32, 33]. Functional annotations that were assigned to fewer than three proteins and with a p-value >0.05 were eliminated from the list. A clear enrichment of proteins of mitochondrial origin was detected, along with enriched biological process terms associated with neuronal development and differentiation (Figure 3b). The significant reduction of one such protein, beta III-tubulin (TBB3), to approximately one third of normal levels in three individual SMA motor neuron cell lines was verified by western blotting (Figure 4a) and is in very close agreement with the iTRAQ ratio (iTRAQ ratio 0.35; Supplementary Table 1a). Immunocytochemistry analysis revealed a global reduction of beta III-tubulin in both cell bodies and cellular processes of SMA motor neurons compared to control motor neurons at the same number of weeks of differentiation (Figure 4b). Whilst the control motor neurons expressed beta III-tubulin at levels of more than four times the amount of that seen in the control genetically matched fibroblasts (iTRAQ ratio of 4.36), beta III-tubulin levels

were not significantly increased in the SMA motor neurons compared to their respective, genetically-matched, fibroblasts (iTRAQ ratio 1.13; not significant). This was despite the fact that motor neuron and pan-neuronal markers were clearly evident and similar in these cells (Figure 1). These findings correlate well with previous work showing a 1.3-1.4 fold reduction in the total number of processes in the SMA motor neurons at late stages of differentiation (i.e. 7 – 10 weeks) compared to control motor neurons[18].

3.4 Ubiquitin carboxyl-terminal esterase L1 is decreased in SMA motor neurons.

Another protein that was implicated in neuronal development (Figure 3b) (that was increased only in control motor neurons vs control fibs), and of some interest already to SMA, is ubiquitin carboxyl-terminal esterase L1 (UCHL1). UCHL1 was among the six proteins that were differentially expressed in one direction (i.e. up- or down-regulated) when SMA fibroblasts were compared to control fibroblasts and then expressed in the opposite direction when SMA motor neurons were compared to CTR motor neurons (Table 1). Levels of UCHL1 appear to be elevated in SMA patient fibroblasts and SMA mouse models[34,35]. Contrary to this, we observed a reduction of UCHL1 levels in SMA motor neurons compared to the control motor neurons by iTRAQ (ratio 0.68; p value 0.049), despite the original SMA fibroblasts containing higher levels than the control fibroblasts (ratio 1.39; p value 0.007) (Supplementary Table 1a, b). This observation was supported by western blot, immunocytochemistry and qPCR analysis. Western blot analysis of UCHL1 protein levels in three individual SMA motor neuron cells lines, compared to three control motor neuron cell lines showed a similar trend (Figure 5a) (ns, p value 0.10; presumably due to the variation between different cell lines). Immunocytochemistry analysis of the 32i SMA motor neurons also indicated lower levels of UCHL1, compared to the 14i control motor neurons (Figure 5b). In addition, a statistically significant reduction by approximately 65% (p value 0.04) of *UCHL1* gene expression was detected in the same three SMA motor neuron cells lines compared to the same control motor neuron cell lines (Figure 5c).

3.5 Ubiquitin-activating enzyme 1 is reduced and differentially localized in SMA motor neurons

Several of the differentially expressed proteins (Supplementary Table 1a, Figure 3) have previously been reported as differentially expressed in SMA, further supporting the validity of these iPS cells as a model for SMA, as well as the overall approach employed in this study. Calreticulin - increased here by 1.89-fold in the SMA motor neurons compared to the control motor neurons (Supplementary Table 1a) - was previously shown to be increased in SMA mouse muscle, SMA fibroblasts and SMA patient muscle biopsies by approximately 1.5-fold, on average, although considerable variability between patients was noted[36]. Mutations in the ubiquitin-activating enzyme 1 (UBA1; previously UBE1) have been reported to cause infantile-onset X-linked spinal muscular atrophy (SMAX2)[37, 38] and the levels of UBA1 were reduced by approximately 50% in SMA mouse spinal cord[33], more than 60% in skeletal muscle[32] and by 50% in SMA mouse Schwann cells[39]. In close agreement with this, we observed a 0.48-fold reduction of UBA1 in the SMA motor neurons compared to the control motor neurons by iTRAQ mass spectrometry (Supplementary Table 1a). This reduction was verified by western

blot analysis of SMA (n=3) and control (n=3) motor neuron cell lines (Figure 6a), by immunocytochemistry in SMI32-positive cells (Figure 6b) and a similar trend was noted by gene-expression analysis of *UBA1* transcript variants 1 and 2 (in the same six cell lines used for western blotting) (Figure 6c). In the control motor neurons, the vast majority of UBA1 was localized to the nucleus and this was in contrast to the mainly cytoplasmic-distribution seen in the SMA motor neurons (Figure 6b), even in cells with relatively high levels of SMI32 expression (4th row, Figure 6b). It seems likely that this represents a developmental abnormality in the SMA motor neurons, since nuclear accumulation of UBA1 appears to correlate with neuronal maturation[34, 40].

4. Discussion

In this study, human iPSC-derived motor neurons were used to identify motor neuron-specific down-stream effects of reduced SMN, not found in fibroblasts, which may help to explain the particular vulnerability of motor neurons in SMA. Here, we provide evidence that motor neurons from SMA patients display abnormalities in developmental and differentiation pathway proteins, and that many of these molecular differences are distinct from those seen in the genetically matched fibroblasts.

A new approach for gaining insight into the molecular pathways involved the dysfunction and demise of motor neurons in SMA has been made possible by the development of iPSC-derived motor neuron models from multiple SMA patients [17,18,41, 42,43]. In addition to displaying the obvious requirements of such a model (including reduced SMN protein and displaying the desired characterisations of diseased motor neurons[17,18]), we have been able to further validate the model via the identification, at the gene and protein level, of downstream consequences of reduced SMN that have been identified in other SMA model systems (e.g. UBA1[34]). Though UBA1 is probably best known as an integral player in the ubiquitin protein-degradation pathway, this cascade also has important regulatory functions for the differentiation, development, and growth of neuronal cells[44,45]. In addition to reduced levels of UBA1, we observed differential distribution within the cells, whereby the majority of UBA1 was localized in the cytoplasm in SMA motor neurons, in contrast to the mainly nuclear distribution seen in control motor neurons. It seems likely that the differential distribution seen in the SMA motor neurons represents a developmental delay or abnormality in these cells since nuclear accumulation of UBA1 correlates with neuronal maturation and differentiation in chick embryos[40] and mouse motor neurons[34]. Further support for this hypothesis comes from a clinical case report highlighting neurodevelopmental abnormalities in an infant with a type of SMA caused by a mutation in the *UBA1* gene (SMAX2)[38]. Wishart et al.[34] reported that nuclear accumulation of UBA1 occurs in control and also SMA mouse motor neurons sometime between postnatal day 3 (P3) and 7, by which time, a reduction of cytoplasmic UBA1 staining intensity was noted in the SMA mice. It will be of interest, in the future, to determine whether the rate of subcellular redistribution of UBA1 differs between SMA and control mice, and in other cell and animal models.

Previous studies have highlighted neuro-developmental defects in SMA in primary tissue from zebrafish, mouse models, post-mortem patient spinal cord, and SMN-depleted germline stem

cells from *Drosophila*[11, 46, 47, 48]. However, many of these studies are limited in the fact that they were conducted using transgenic animal models or in late-symptomatic SMA patients. Little is known, therefore, about the precise molecular pathway(s) underlying the series of events that lead to these abnormalities *in vivo* and how well these models reflect the disease aetiology seen early on in SMA patients. The expression of beta III-tubulin is well-known to be associated with differentiation and decreased cell proliferation of neurons[49]. Neural stem cells (NSCs) from a mouse model of very severe SMA produce fewer beta III-tubulin -positive cells, and those that are produced, have fewer and shorter neurites; suggestive of neurodevelopmental abnormalities[50]. Such an observation, however, has never been confirmed in quantitative manner in SMA patient-derived neurons. Here we describe a global reduction of beta III-tubulin protein levels by iTRAQ, western blotting and immunocytochemistry in SMA motor neurons. Alongside the reduction of beta III-tubulin -positive cells, Shafey et al.[50] also observed an increase in the numbers of proliferative NSCs and nestin-positive cells; implying that these cells had not differentiated as they ought to[50].

The observation that UCHL1 and other proteins associated with neuronal differentiation and development were reduced in SMA motor neurons compared to control motor neurons supports the hypothesis that aberrations in early neurodevelopmental pathway proteins play a key role in SMA pathogenesis. Although levels of UCHL1 are increased in SMA patient fibroblasts (Supplementary Table 1, [35]) and in mouse models[34, 52], our results indicate that UCHL1 occurs at lower levels in SMA motor neurons compared to control motor neurons. Though this is the first such observation, it is not so surprising when we consider what we know already about the role of UCHL1 in neurons. In addition to an essential role maintaining the structure and function of the mouse neuromuscular junction[53], patients with a loss-of-function mutation in *UCHL1* demonstrate early-onset progressive neurodegeneration[54], and more recently, UCHL1 was shown to have a role in maintaining the viability of corticospinal motor neurons[55]. Moreover, pharmacological inhibition of UCHL1 appears to exacerbate disease symptoms in a mouse model of SMA, suggesting that the increased levels seen in certain cell types may either be due to an attempted compensatory response or that these cells respond differently to reduced SMN, compared to motor neurons[51]. This finding also highlights the potential complexities of therapies for SMA aimed at restoring ubiquitin homeostasis[34, 52].

In a recent article by Hornburg et al.[20], proteomics analysis was used to delineate differences between primary and cell line mouse models of motor neuron disease. The study placed neuronal cell line models halfway between primary motor neurons and unrelated cell lines, in terms of the proteomic-profile of the cells. Although it is not possible to directly compare the proteome of primary human motor neurons with iPSC-derived motor neurons in a similar fashion, our results suggest that the motor neurons used in this study are far removed from their genetically matched fibroblasts, at least in terms of their proteomic profile. When SMA motor neurons were compared to control motor neurons, all but one of the 99 differentially expressed proteins were distinct from the differences seen when genetically matched fibroblast cell lines were compared. The differential expression of several of these candidates that have been implicated in SMA (i.e. SMN, beta III-tubulin and UBA1) have been verified here in three separate control and SMA iPS cell lines. Our results validate the potential of iPSC technology in identifying relevant disease mechanisms in motor neuron diseases by a proteomics approach and builds upon iPSC disease modeling studies that have been limited by number of independent (non-clonal) diseased patient

cell lines[56-61]. In the future, it will be interesting to examine this further by label-free quantitative analysis of a larger cohort of patient-derived samples and to characterise the molecular implications of genetic diversity / heterogeneity of the cell lines.

Despite recent advances in our understanding of the molecular pathways involved in SMA[62], it is still not clear why lower motor neurons, in particular, are so vulnerable to reduced levels of SMN protein. Though previous longitudinal analyses suggests that both SMA and control iPS-derived motor neuron cultures undergo neurogenesis at similar levels over time[18], it is conceivable that some proteomic differences identified here could reflect a delay in development that may not be apparent at a later stage, if the cells were able to "catch up" developmentally. It is important to consider, however, that a delay in any aspect of motor neuron development could itself be a fundamental difference with catastrophic consequences for motor neuron circuitry development. As such, if any proteomic changes are due to a slower development speed, they are still likely to be highly relevant to SMA. This notion is supported by the fact that early postnatal delivery of AAV9-SMN rescues the SMA mouse, while later delivery does not[63], indicating that there is a critical developmental time window.

The distinctly different patterns of differential expression seen here between SMA and control motor neurons, compared to the differential expression seen in genetically matched fibroblasts, indicates that SMN depletion has very different downstream consequences in different cell types. The proteomic differences identified here, therefore, are likely to provide a useful resource for exploring the molecular consequences of reduced SMN in motor neurons and for the identification of novel therapeutic targets for SMA. In particular, the robust finding here, of depleted levels of UBA1 in iPSC-derived motor neurons from three separate SMA patients compared to controls, supports a growing body of evidence[34,37,38] to suggest that this protein is likely to be a major contributor to pathogenesis in SMA.

Author contributions

HRF participated in the study design, conducted experiments, analyzed data, and wrote the manuscript. SS and CB conducted the mass spectrometry analysis. BM performed differentiation and culturing of the iPS cells. ARG performed the qRT-PCR experiments. GEM participated in the study design and provided reagents for the study. DS wrote manuscript, participated in the study design, conducted iPS cell characterization, neuronal differentiation experiments and analyzed data. The manuscript was written through contributions of all authors. All authors have given approval to the final version of the manuscript.

Acknowledgments

This work was supported by The RJAH Institute of Orthopaedics, UK (H.F.), The SMA Trust, UK (H.F.), Cedars-Sinai Institutional startup funds (D.S), California Institute for Regenerative Medicine Grant RT-02040 (D.S.), National Center for Advancing Translational Sciences (NCATS), Grant UL1TR000124 (D.S.), and the Wellcome Trust [grant number 094476/Z/10/Z] which funded the purchase of the TripleTOF 5600 mass spectrometer at the BSRC Mass

Spectrometry and Proteomics Facility, University of St Andrews (S.S. and C.B.). D.S. is also supported by funds from National Institute of Health (NINDS) grant U54NS091046. The funders had no role in study design, data collection and analysis, decision to publish, or preparation of the manuscript.

References

(1) Lefebvre S, Bürglen L, Reboullet S, Clermont O, Burlet P, Viollet L, Benichou B, Cruaud C, Millasseau P, Zeviani M. Identification and characterization of a spinal muscular atrophy-determining gene. *Cell* (1995) **80**: 155-165.

(2) Lorson CL, Strasswimmer J, Yao JM, Baleja JD, Hahnen E, Wirth B, Le T, Burghes AH, Androphy EJ. SMN oligomerization defect correlates with spinal muscular atrophy severity. *Nat Genet* (1998) **19**: 63-6.

(3) Pellizzoni L, Charroux B, Dreyfuss G. SMN mutants of spinal muscular atrophy patients are defective in binding to snRNP proteins. *Proc Natl Acad Sci U S* (1999) **96**: 11167-72.

(4) Lefebvre S, Burlet P, Liu Q, Bertrandy S, Clermont O, Munnich A, Dreyfuss G, Melki J. *Nat Genet* (1997) **16**: 265–9.

(5) Coovert DD, Le TT, McAndrew PE, Strasswimmer J, Crawford TO, Mendell JR, Coulson SE, Androphy EJ, Prior TW, Burghes AH. The survival motor neuron protein in spinal muscular atrophy. *Hum Mol Genet* (1997) **6**: 1205-14.

(6) Pellizzoni L, Kataoka N, Charroux B and Dreyfuss G. A novel function for SMN, the spinal muscular atrophy disease gene product, in pre-mRNA splicing. *Cell* (1998) **95**: 615-624.

(7) Rossoll W, Jablonka S, Andreassi C, Kröning AK, Karle K, Monani UR, Sendtner M. Smn, the spinal muscular atrophy-determining gene product, modulates axon growth and localization of beta-actin mRNA in growth cones of motoneurons. *J Cell Biol* (2003) **163**: 801-812.

(8) Carrel TL, McWhorter ML, Workman E, Zhang H, Wolstencroft EC, Lorson C, Bassell GJ, Burghes AH and Beattie CE. Survival motor neuron function in motor axons is independent of functions required for small nuclear ribonucleoprotein biogenesis. *J Neurosci* (2006) **26**: 11014-22.

(9) Kariya S, Park GH, Maeno-Hikichi Y, Leykekhman O, Lutz C, Arkovitz MS, Landmesser LT, Monani UR. Reduced SMN protein impairs maturation of the neuromuscular junctions in mouse models of spinal muscular atrophy. *Hum Mol Genet* (2008) **17**: 2552–69.

(10) Burghes AH, Beattie CE. Spinal muscular atrophy: why do low levels of survival motor neuron protein make motor neurons sick? *Nat Rev Neurosci* (2009) **10**: 597–609.

(11) Murray LM, Sheena L, Bäumer D, Parson SH, Talbot K, Gillingwater TH. Pre-symptomatic development of lower motor neuron connectivity in a mouse model of severe spinal muscular atrophy. *Hum Mol Genet* (2010) **19**: 420-433.

(12) Sleigh JN, Gillingwater TH, Talbot K. The contribution of mouse models to understanding the pathogenesis of spinal muscular atrophy. *Dis Model Mech* (2011) **4**: 457-67.

(13) Hamilton G, Gillingwater TH. Spinal muscular atrophy: going beyond the motor neuron. *Trends Mol Med* (2013) **19**: 40-50.

(14) Edens BM, Ajroud-Driss S, Ma L, Ma YC. Molecular mechanisms and animal models of spinal muscular atrophy. *Biochim Biophys Acta* (2015) **1852**: 685-692.

(15) Takahashi K, Tanabe K, Ohnuki M, Narita M, Ichisaka T, Tomoda K, Yamanaka S. Induction of pluripotent stem cells from adult human fibroblasts by defined factors. *Cell* (2007) **131**: 861-72.

(16) Yu J, Vodyanik MA, Smuga-Otto K, Antosiewicz-Bourget J, Frane JL, Tian S, Nie J, Jonsdottir GA, Ruotti V, Stewart R, Slukvin II, Thomson JA. Induced pluripotent stem cell lines derived from human somatic cells. *Science* (2007) **318**: 1917-20.

(17) Ebert AD, Svendsen CN. Stem cell model of spinal muscular atrophy. *Arch Neurol* (2010) **67**: 665–669.

(18) Sareen D, Ebert AD, Heins BM, McGivern JV, Ornelas L, Svendsen CN. Inhibition of apoptosis blocks human motor neuron cell death in a stem cell model of spinal muscular atrophy. *PLoS One* (2012) **7**: e39113.

(19) Barrett R, Ornelas L, Yeager N, Mandefro B, Sahabian A, Lenaeus L, Targan SR, Svendsen CN, Sareen D. Reliable generation of induced pluripotent stem cells from human lymphoblastoid cell lines. *Stem Cells Transl Med* (2014) **3**: 1429-34.

(20) Hornburg D, Drepper C, Butter F, Meissner F, Sendtner M, Mann M. Deep proteomic evaluation of primary and cell line motoneuron disease models delineates major differences in neuronal characteristics. *Mol Cell Proteomics* (2014) **13**: 3410-20.

(21) Sareen D, O'Rourke JG, Meera P, Muhammad AK, Grant S, Simpkinson M, Bell S, Carmona S, Ornelas L, Sahabian A, Gendron T, Petrucelli L, Baughn M, Ravits J, Harms MB, Rigo F, Bennett CF, Otis TS, Svendsen CN, Baloh RH. Targeting RNA foci in iPSC-derived motor neurons from ALS patients with a C9ORF72 repeat expansion. *Sci Transl Med* (2013) **5**: (208), 208ra149.

(22) Sareen D, Gowing G, Sahabian A, Staggenborg K, Paradis R, Avalos P, Latter J, Ornelas L, Garcia L, Svendsen CN. Human induced pluripotent stem cells are a novel source of neural progenitor cells (iNPCs) that migrate and integrate in the rodent spinal cord. *J Comp Neurol* (2014) **522**: 2707-28.

(23) Müller FJ, Brändl B, Loring JF. *StemBook* (2008-2012) Cambridge (MA): Harvard Stem Cell Institute.

(24) Chambers SM, Fasano CA, Papapetrou EP, Tomishima M, Sadelain M, Studer L. Highly efficient neural conversion of human ES and iPS cells by dual inhibition of SMAD signaling. *Nat Biotechnol.* (2009) **27**: 275-80.

(25) Svendsen CN, ter Borg MG, Armstrong RJ, Rosser AE, Chandran S, Ostenfeld T, Caldwell MA. A new method for the rapid and long term growth of human neural precursor cells. *J Neurosci Methods* (1998) **85**: 141-52.

(26) Fuller HR, Slade R, Jovanov-Milosevic N, Babic M, Sedmak G, Simic G, Fuszard MA, Shirran SL, Botting CH and Gates MA. Stathmin is highly enriched in the developing corticospinal tract. Molecular and Cellular Neuroscience (2015) **69:** 12-21.

(27) Eaton SL1, Roche SL, Llavero Hurtado M, Oldknow KJ, Farquharson C, Gillingwater TH, Wishart TM. Total protein analysis as a reliable loading control for quantitative fluorescent Western blotting. PLoS One (2013) e72457. doi: 10.1371/journal.pone.0072457

(28) Schmittgen TD, Livak KJ. Analyzing real-time PCR data by the comparative C(T) method. *Nat Protoc* (2008) **3***:* 1101-8.

(28) Livak KJ, Schmittgen TD. Analysis of relative gene expression data using real-time quantitative PCR and the 2(-Delta Delta C(T)) Method. *Methods* (2001) **25**: 402-8.

(29) Fuller HR, Man NT, Lam le T, Shamanin VA, Androphy EJ, Morris GE. Valproate and bone loss: iTRAQ proteomics show that valproate reduces collagens and osteonectin in SMA cells. *J Proteome Res* (2010) **9**: 4228-33.

(30) Hao LT, Fuller HR, Lam TL, Thanh LT, Burghes AHM, Morris GE. Absence of gemin5 from SMN complexes in nuclear Cajal bodies. *BMC Cell Biology* (2007) **8:** 28.

(31) Huang DW, Sherman BT, Lempicki RA. Systematic and integrative analysis of large gene lists using DAVID Bioinformatics Resources. *Nature Protoc* (2009) **4**: 44-57.

(32) Huang DW, Sherman BT, Lempicki RA. Bioinformatics enrichment tools: paths toward the comprehensive functional analysis of large gene lists. *Nucleic Acids Res* (2009) **37**: 1-13.

(33) Wishart TM, Mutsaers CA, Riessland M, Reimer MM, Hunter G, Hannam ML, Eaton SL, Fuller HR, Roche SL, Somers E, Morse R, Young PJ, Lamont DJ, Hammerschmidt M, Joshi A, Hohenstein P, Morris GE, Parson SH, Skehel PA, Becker T, Robinson IM, Becker CG, Wirth B, Gillingwater TH. Dysregulation of ubiquitin homeostasis and β-catenin signaling promote spinal muscular atrophy. *J Clin Invest* (2014) **124**: 1821-34.

(34) Hsu SH, Lai MC, Er TK, Yang SN, Hung CH, Tsai HH, Lin YC, Chang JG, Lo YC, Jong YJ. Ubiquitin carboxyl-terminal hydrolase L1 (UCHL1) regulates the level of SMN expression through ubiquitination in primary spinal muscular atrophy fibroblasts. *Clin Chim Acta* (2010) **411**: 1920-8.

(35) Mutsaers CA, Lamont DJ, Hunter G, Wishart TM, Gillingwater TH. Label-free proteomics identifies Calreticulin and GRP75/Mortalin as peripherally accessible protein biomarkers for spinal muscular atrophy. *Genome Med* (2013) **5**: 95.

(36) Ramser J, Ahearn ME, Lenski C, Yariz KO, Hellebrand H, von Rhein M, Clark RD, Schmutzler RK, Lichtner P, Hoffman EP, Meindl A, Baumbach-Reardon L. Rare missense and synonymous variants in UBE1 are associated with X-linked infantile spinal muscular atrophy. *Am J Hum Genet* (2008) **82**: 188-93.

(37) Dlamini N, Josifova DJ, Paine SM, Wraige E, Pitt M, Murphy AJ, King A, Buk S, Smith F, Abbs S, Sewry C, Jacques TS, Jungbluth H. Clinical and neuropathological features of X-linked spinal muscular atrophy (SMAX2) associated with a novel mutation in the UBA1 gene. *Neuromuscul Disord* (2013) **23**: 391-8.

(38) Aghamaleky Sarvestany A, Hunter G, Tavendale A, Lamont DJ, Llavero Hurtado M, Graham LC, Wishart TM, Gillingwater TH. Label-free quantitative proteomic profiling identifies disruption of ubiquitin homeostasis as a key driver of Schwann cell defects in spinal muscular atrophy. *J Proteome Res* (2014) **13**: 4546-57.

(39) Smith-Thomas LC, Kent C, Mayer RJ, Scotting PJ. Protein ubiquitination and neuronal differentiation in chick embryos. *Brain Res Dev Brain Res* (1994) **81**: 171-7.

(40) Yoshida M, Kitaoka S, Egawa N, Yamane M, Ikeda R, Tsukita K, Amano N, Watanabe A, Morimoto M, Takahashi J, Hosoi H, Nakahata T, Inoue H, Saito M.K. Modeling the early phenotype at the neuromuscular junction of spinal muscular atrophy using patient-derived iPSCs. *Stem Cell Reports* (2015) **4**: 561-8.

(41) Corti S, Nizzardo M, Simone C, Falcone M, Nardini M, Ronchi D, Donadoni C, Salani S, Riboldi G, Magri F, Menozzi G, Bonaglia C, Rizzo F, Bresolin N, Comi GP. Genetic correction of human induced pluripotent stem cells from patients with spinal muscular atrophy. *Sci Transl Med* (2012) **4**: 165ra162.

(42) Chang T, Zheng W, Tsark W, Bates S, Huang H, Lin RJ, Yee JK. Brief report: phenotypic rescue of induced pluripotent stem cell-derived motoneurons of a spinal muscular atrophy patient. *Stem Cells* (2011) **29**: 2090-3.

(43) Hamilton AM, Zito K. Breaking it down: the ubiquitin proteasome system in neuronal morphogenesis. *Neural Plast* (2013), 196848.

(44) Saritas-Yildirim B, Silva EM. The role of targeted protein degradation in early neural development. *Genesis* (2014) **52**: 287-99.

(45) Hao le T, Duy PQ, Jontes JD, Beattie CE. Motoneuron development influences dorsal root ganglia survival and Schwann cell development in a vertebrate model of spinal muscular atrophy. *Hum Mol Genet* (2015) **24**: 346-60.

(46) Simic G, Mladinov M, Simic DS, Jovanov Milosevic N, Islam A, Pajtak A, Barisic N, Sertic J, Lucassen PL, Hof PR, Kruslin B. Abnormal motoneuron migration, differentiation, and axon outgrowth in spinal muscular atrophy. *Acta Neuropathol* (2008) **115**: 313-26.

(47) Grice SJ, Liu JL. Survival motor neuron protein regulates stem cell division, proliferation, and differentiation in Drosophila. *PLoS Genet* (2011) **7**: e1002030.

(48) Katsetos CD, Legido A, Perentes E, Mörk SJ. Class III beta-tubulin isotype: a key cytoskeletal protein at the crossroads of developmental neurobiology and tumor neuropathology. *J Child Neurol* (2003) **18**: 851-66.

(49) Shafey D, MacKenzie AE, Kothary R. Neurodevelopmental abnormalities in neurosphere-derived neural stem cells from SMN-depleted mice. *J Neurosci Res* (2008) **86:** 2839-47.

(50) Wiese C, Rolletschek A, Kania G, Blyszczuk P, Tarasov KV, Tarasova Y, Wersto RP, Boheler KR, Wobus AM. Nestin expression--a property of multi-lineage progenitor cells? *Cell Mol Life Sci* (2004) **61**: 2510-22.

(51) Powis RA, Mutsaers CA, Wishart TM, Hunter G, Wirth B, Gillingwater TH. Increased levels of UCHL1 are a compensatory response to disrupted ubiquitin homeostasis in spinal muscular atrophy and do not represent a viable therapeutic target. *Neuropathol Appl Neurobiol* (2014) **40**: 873-87.

(52) Chen F, Sugiura Y, Myers KG, Liu Y, Lin W. Ubiquitin carboxyl-terminal hydrolase L1 is required for maintaining the structure and function of the neuromuscular junction. *Proc Natl Acad Sci USA* (2010) **107**: 1636-1641.

(53) Bilguvar K, Tyagi NK, Ozkara C, Tuysuz B, Bakircioglu M, Choi M, Delil S, Caglayan AO, Baranoski JF, Erturk O, Yalcinkaya C, Karacorlu M, Dincer A, Johnson MH, Mane S, Chandra SS, Louvi A, Boggon TJ, Lifton RP, Horwich AL, Gunel M. Recessive loss of function of the neuronal ubiquitin hydrolase UCHL1 leads to early-onset progressive neurodegeneration. *Proc Natl Acad Sci U S A* (2013) **110**: 3489-94.

(54) Jara JH, Genç B, Cox GA, Bohn MC, Roos RP, Macklis JD, Ulupınar E, Özdinler PH. Corticospinal Motor Neurons Are Susceptible to Increased ER Stress and Display Profound Degeneration in the Absence of UCHL1 Function. *Cereb Cortex* (2015) Jan 16. pii: bhu318.

(55) Shan B, Xu C, Zhang Y, Xu T, Gottesfeld JM, Yates JR 3rd. Quantitative proteomic analysis identifies targets and pathways of a 2-aminobenzamide HDAC inhibitor in Friedreich's ataxia patient iPSC-derived neural stem cells. *J Proteome Res* (2014) **3**: 4558-66.

(56) Boza-Morán MG, Martínez-Hernández R, Bernal S, Wanisch K, Also-Rallo E, Le Heron A, Alías L, Denis C, Girard M, Yee JK, Tizzano EF, Yáñez-Muñoz RJ. Decay in survival motor neuron and plastin 3 levels during differentiation of iPSC-derived human motor neurons. *Sci Rep* (2015) **5**:11696.

(57) Chen H, Qian K, Du Z, Cao J, Petersen A, Liu H, Blackbourn LW 4th, Huang CL, Errigo A, Yin Y, Lu J, Ayala M, Zhang SC. Modeling ALS with iPSCs reveals that mutant SOD1 misregulates neurofilament balance in motor neurons. *Cell Stem Cell* (2014) **14**:796-809.

(58) Donnelly CJ, Zhang PW, Pham JT, Haeusler AR, Mistry NA, Vidensky S, Daley EL, Poth EM, Hoover B, Fines DM, Maragakis N, Tienari PJ, Petrucelli L, Traynor BJ, Wang J, Rigo F, Bennett CF, Blackshaw S, Sattler R, Rothstein JD. RNA toxicity from the ALS/FTD C9ORF72 expansion is mitigated by antisense intervention. *Neuron* (2013) **80**:415-28.

(59) Bilican B, Serio A, Barmada SJ, Nishimura AL, Sullivan GJ, Carrasco M, Phatnani HP, Puddifoot CA, Story D, Fletcher J, Park IH, Friedman BA, Daley GQ, Wyllie DJ, Hardingham GE, Wilmut I, Finkbeiner S, Maniatis T, Shaw CE, Chandran S. Mutant induced pluripotent stem cell lines recapitulate aspects of TDP-43 proteinopathies and reveal cell-specific vulnerability. *PNAS* (2012) **109**: 5803-8.

(60) Corti S1, Nizzardo M, Simone C, Falcone M, Nardini M, Ronchi D, Donadoni C, Salani S, Riboldi G, Magri F, Menozzi G, Bonaglia C, Rizzo F, Bresolin N, Comi GP. Genetic correction of human induced pluripotent stem cells from patients with spinal muscular atrophy. *Science translational medicine* (2012) **4**: 165ra162.

(61) d'Ydewalle C, Sumner CJ. Spinal Muscular Atrophy Therapeutics: Where do we Stand? *Neurotherapeutics* (2015) **12**: 303-16.

(62) Foust KD, Wang X, McGovern VL, Braun L, Bevan AK, Haidet AM, Le TT, Morales PR, Rich MM, Burghes AH, Kaspar BK. Rescue of the spinal muscular atrophy phenotype in a mouse model by early postnatal delivery of SMN. *Nat Biotechnol* (2010) **28**: 271-4.

Table 1. Differentially-expressed proteins with opposite expression levels in SMA fibroblasts compared to SMA motor neurons from the same patient.
Differentially-expressed proteins that were changed in one direction (i.e. up- or down- regulated) when SMA fibroblasts were compared to control fibroblasts, but changed in the opposite direction when SMA motor neurons were compared to control motor neurons. Only statistically significant differential expression (i.e. those with p values of <0.05) are shown. Abbreviations in column headings refer to the following: protein name = given name in Swiss-Prot database; [n] = number of unique peptides used for quantification; fibs = fibroblasts; SMA MNs = 32i motor neurons; CTR MNs = 14i control motor neurons.

Protein Name	Accession number	Sequence coverage (%)	Avg. iTRAQ ratio (SMA fibs/ CTR fibs)	Avg. iTRAQ ratio (SMA MNs/ CTR iMNs)

Myosin-3	P11055	52.5 [122]	0.75	5.95
Caldesmon	Q05682	42.0 [23]	0.71	1.92
Zyxin	Q15942	27.1 [18]	0.72	1.47
Synaptopodin-2	Q9UMS6	10.0 [3]	0.66	1.38
UCHL1	P09936	56.1 [37]	1.40	0.68
CNP	P09543	30.6 [3]	1.41	0.54

Figure 1: Characterization of iPSC line and neuronal cultures representative of a healthy control and SMA Type 1 patient iPSC line.
(A) Representative positive immunostaining for nuclear and surface pluripotency antigens with normal G-band karyotype of the iPS cells shown at the right. (B) Gene-chip and bioinformatics based PluriTest characterization of control and SMA iPS cell lines used in this study. H9 human embryonic stem cells (hESCs) were used as positive control, while human dermal fibroblasts and primary human neural progenitor cells (hNPCs) were negative controls. (C) Upon neuronal induction and differentiation to the cultures analyzed contain: few Nestin progenitors (<10%) and Map2 a/b neurons (dendritic marker), pan-neurons marker beta III-tubulin (>60%) with few astroglial (GFAP) cells, mostly SMI32- and ISL1 (Islet-1) positive motor neurons (~40%). Nkx6.1 and ChAT are spinal motor neuron markers that are expressed in both control and SMA –derived motor neurons. Scale bar for A is 75 µm. Scale bar for C is 200 µm. (D) Representative western blot showing SMN protein levels in three different control and SMA motor neuron cell lines, along with Coomassie stained gel as loading control. The graph represents mean integrated density of SMN bands from this blot / total protein (Coomassie gel), as determined by ImageJ software. Error bars represent standard error from the mean and statistical significance was calculated using an unpaired, 1-tailed t-test with two-sample unequal variance. Please note that the Coomassie loading control shown here is the same that is shown for Figure 4a because they were both derived from the same blot. (E) Average gene expression levels of full-length (FL)-*SMN* in the control and SMA motor neurons (the same six cell lines shown in (D)), as determined by qRT-PCR ($p = 0.002$; unpaired, one-tailed t-test). Relative fold expression was normalized to H9 hESCs. Error bars represent standard error from the mean

Figure 2: SMN depletion has contrasting downstream effects on the proteome of motor neurons compared to genetically matched fibroblasts
While 99 proteins were differentially expressed with statistical significance when SMA motor neurons (n=1) were quantitatively compared to control motor neurons (n=1) (A), only 18 proteins were differentially expressed when SMA fibroblasts (n=1) were quantitatively compared to control fibroblasts (n=1) (B). Of one these 18 proteins, only one was also differentially expressed in the same direction with statistical significance when the SMA MNs were compared to control MNs, and six of the 18 proteins were differentially expressed in one direction (i.e. up- or down-regulated) when SMA fibroblasts were compared to control fibroblasts and then expressed in the opposite direction when SMA MNs were compared to control MNs (C) (arrows indicate proteins that were verified biochemically). Plots in A and B were generated using using Advaita Bio's iPathwayGuide (http://www.advaitabio.com/ipathwayguide) and plot C was generated using Plotly software (Plotly Technologies Inc. (2015), https://plot.ly).

Figure 3. Perturbation of developmental and differentiation pathways in SMA motor neurons

(A) A Venn diagram and bar chart illustrates the number of differentially expressed proteins seen in control motor neurons (n=1) compared to control fibroblasts (n=1) (blue circle and blue bars) and SMN motor neurons (n=1) compared SMA fibroblasts (n=1) (green circle and green bars). (B) Bioinformatics analysis of the 46 proteins that were only increased in the control motor neurons vs control fibs was conducted using the Database for Annotation, Visualization and Integrated Discovery (DAVID). CTR = control, MNs = motor neurons.

Figure 4. Reduction of beta III-tubulin levels in SMA motor neurons

(A) Representative western blot showing beta III-tubulin protein levels in three different control and SMA motor neuron cell lines, along with Coomassie stained gel as loading control. The graph above it illustrates the average integrated density of the beta III-tubulin bands from this blot / total protein (Coomassie gel), as determined by ImageJ software. Error bars represent standard error from the mean and statistical significance was calculated using an unpaired, 1-tailed t-test with two-sample unequal variance. Please note that the Coomassie loading control shown here is the same that is shown for Figure 1d because they were both derived from the same blot. (B) Representative confocal images indicate a reduction of beta III-tubulin levels in SMI-32 positive 32i SMA motor neurons. CTR = control, MNs = motor neurons.

Figure 5. Decreased UCHL1 levels in SMA motor neurons

(A) Representative western blot showing UCHL1 protein levels in three different control and SMA motor neuron cell lines. The graph above it shows the integrated density of the UCHL1 bands from this blot / total protein (Coomassie gel), as determined by ImageJ software. The graph to the right shows the average integrated density of the UCHL1 bands from this blot / total protein (Coomassie gel). Error bars represent standard error from the mean and statistical significance was calculated using an unpaired, 1-tailed t-test with two-sample unequal variance. (B) Representative confocal images indicate a reduction of UCHL1 levels in SMI32 positive cells. (C) Average gene expression levels of *UCHL1* in the control and SMA motor neuron cell lines (the same six cell lines shown in (A)), as determined by qRT-PCR ($p = 0.04$; unpaired, one-tailed t-test). Relative fold expression was normalized to H9 hESCs. Error bars represent standard error from the mean. CTR = control, MNs = motor neurons.

Figure 6: Reduction and differential localization of UBA1 in SMA motor neurons

(A) Representative western blot showing UBA1 protein levels in three different control and SMA motor neuron cell lines, along with Coomassie stained gel as loading control. The graph illustrates the average integrated density of the UBA1 bands from this blot / total protein (Coomassie gel), as determined by ImageJ software. Error bars represent standard error from the mean and statistical significance was calculated using an unpaired, 1-tailed t-test with two-sample unequal variance. (B) Representative confocal images indicate a reduction of UBA1 levels in SMI32 positive 32i SMA motor neurons and mostly cytoplasmic distribution (in comparison to the mostly nuclear distribution seen in the 14i control (CTR) motor neurons). (C) Average gene expression levels of *UBA1* transcript variants 1 (TV1) ($p = 0.14$; unpaired, one-

1012 tailed t-test) and 2 (TV2) (p=0.08; unpaired, one-tailed t-test) in the control and SMA motor
1013 neuron cell lines (the same six patient and control cell lines shown in (A)), as determined by
1014 qRT-PCR. Relative fold expression was normalized to H9 hESCs. Error bars represent standard
1015 error from the mean. CTR = control, MNs = motor neurons.
1016
1017 **Supplementary information**
1018
1019 **Supplementary File 1, containing:**
1020 S1. Antibodies used for immunocytochemistry and immunoblotting.
1021 S2. Origin, clinical history and genetics of each cell line.
1022 S3. qRT-PCR primers.
1023 S4. Quantitative western blot showing a reduction of gemin2 in SMA motor neurons.
1024 S5. Immunofluorescence staining of iPS-derived motor neurons and fibroblasts.
1025
1026 **Supplementary Table 1:** A protein summary for all the proteins that were identified by iTRAQ-
1027 mass spectrometry with a Protein Threshold (Unused ProtScore (conf)) > 0.05.
1028
1029 **Supplementary Table 2.** A protein summary for the proteins that were differentially expressed
1030 when motor neurons were quantitatively compared, using iTRAQ mass spectrometry, to the
1031 fibroblast lines from which they were derived.
1032
1033

Figure 1.TIF

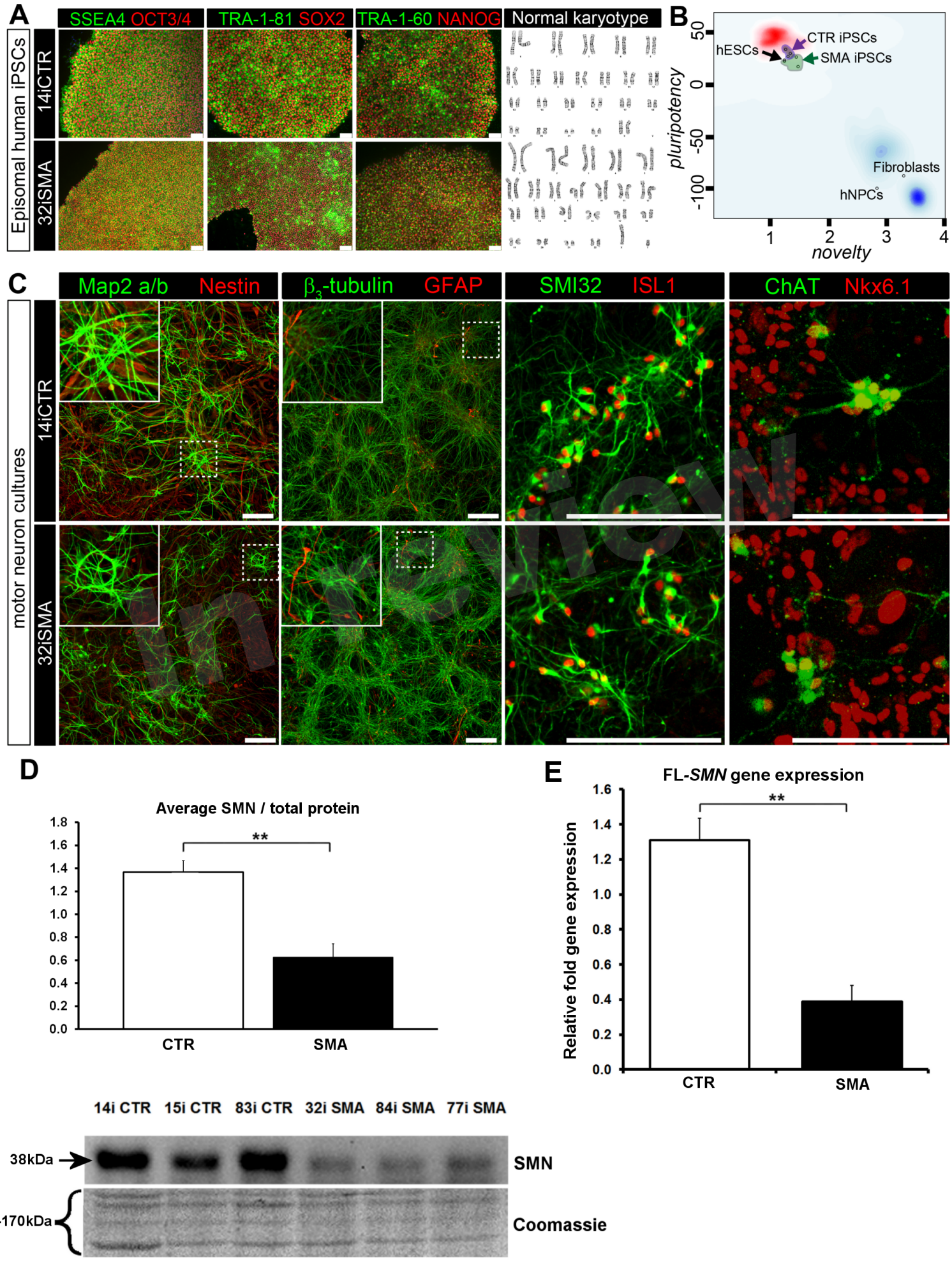
A
SSEA4 OCT3/4
TRA-1-81 SOX2
TRA-1-60 NANOG
Normal karyotype
Episomal human iPSCs
14iCTR
32iSMA
B
CTR iPSCs
hESCs
SMA iPSCs
Fibroblasts
hNPCs
pluripotency
novelty
C
Map2 a/b
Nestin
β3-tubulin
GFAP
SMI32
ISL1
ChAT
Nkx6.1
motor neuron cultures
14iCTR
32iSMA
D
Average SMN / total protein
CTR
SMA
E
FL-SMN gene expression
Relative fold gene expression
CTR
SMA
14i CTR
15i CTR
83i CTR
32i SMA
84i SMA
77i SMA
38kDa
SMN
130-170kDa
Coomassie

Figure 2.TIF

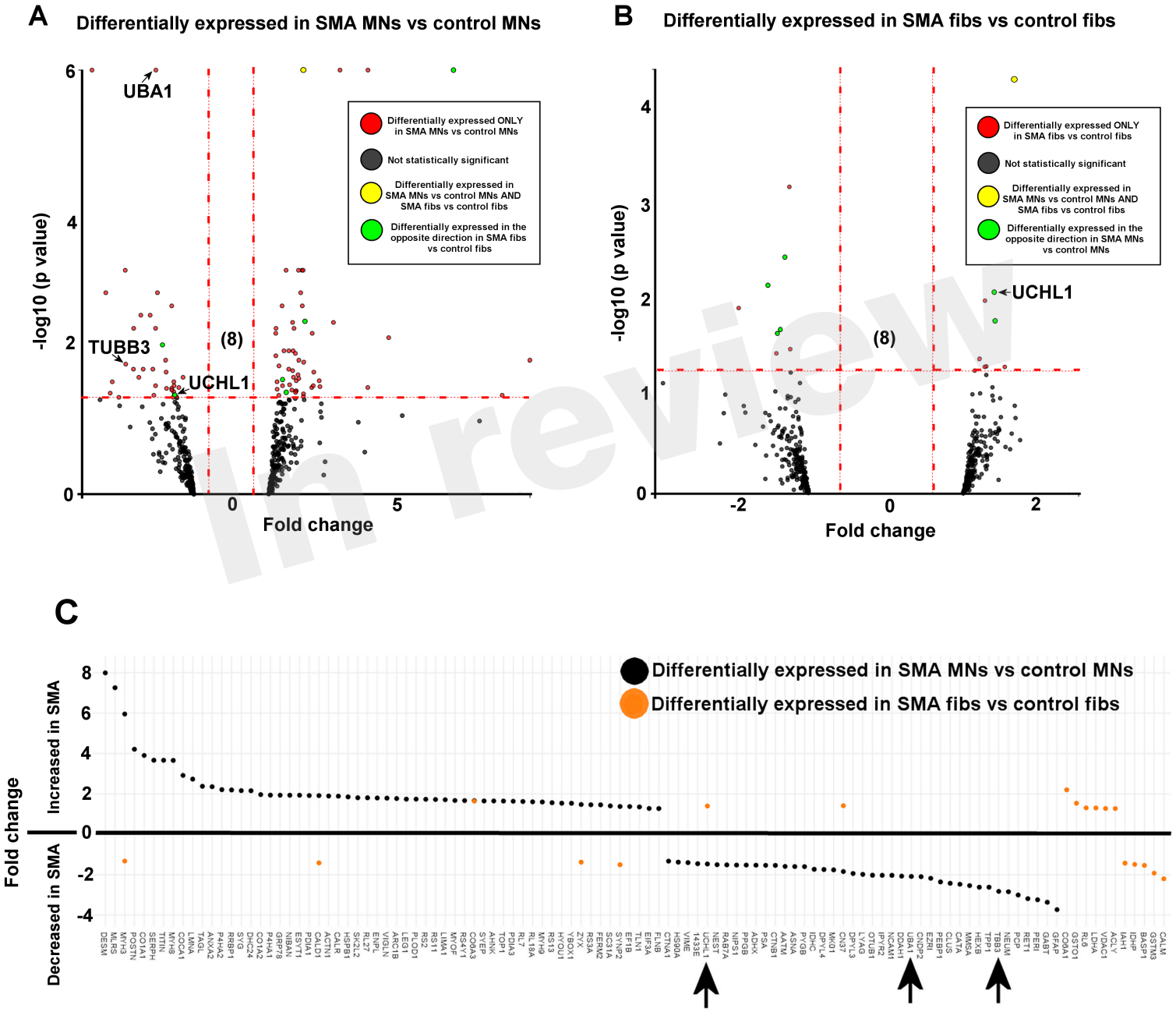

Figure 3.TIF

A

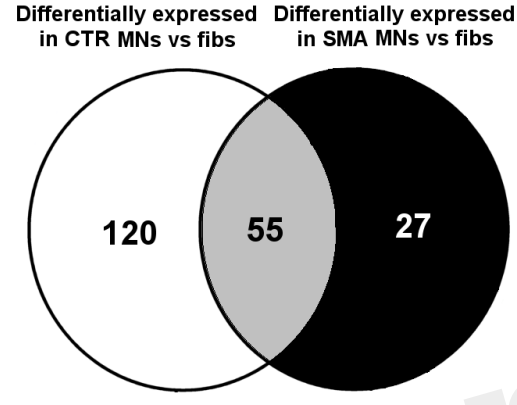

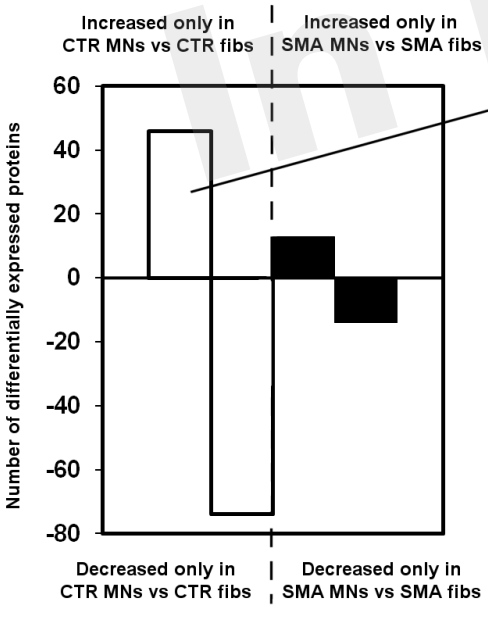

B

Cellular compartment	P_Value	Proteins
mitochondrial matrix	6.80E-06	GABT, ATPB, ACON, AATM, ECHA, LPPRC, MDHM, VDAC1
mitochondrial lumen	6.80E-06	GABT, ATPB, ACON, AATM, ECHA, LPPRC, MDHM, VDAC1
mitochondrial part	8.90E-05	NNTM, PEBP1, GABT, ATPB, ACON, AATM, ECHA, LPPRC, MDHM, VDAC1
mitochondrial nucleoid	1.30E-04	ATPB, ECHA, LPPRC, VDAC1

Biological process	P_Value	Proteins
neuron projection development	1.30E-04	CN37, CLUS, DPYL5, NEUM, MAP2, PTN11, UCHL1
neuron differentiation	3.60E-04	TBB3, CN37, CLUS, DPYL5, NEUM, MAP2, PTN11, UCHL1
neuron projection morphogenesis	4.90E-04	CN37, CLUS, DPYL5, NEUM, PTN11, UCHL1
neuron development	5.80E-04	CN37, CLUS, DPYL5, NEUM, MAP2, PTN11, UCHL1

Figure 4.TIF

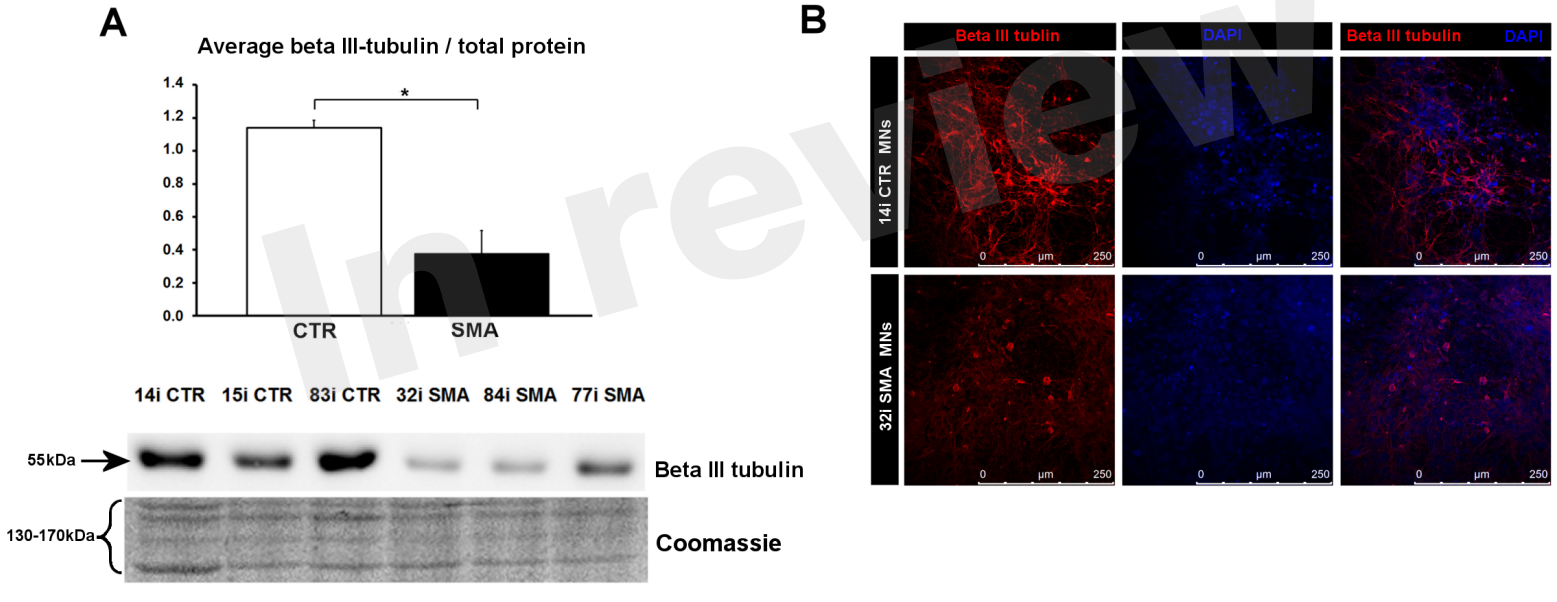

Figure 5.TIF

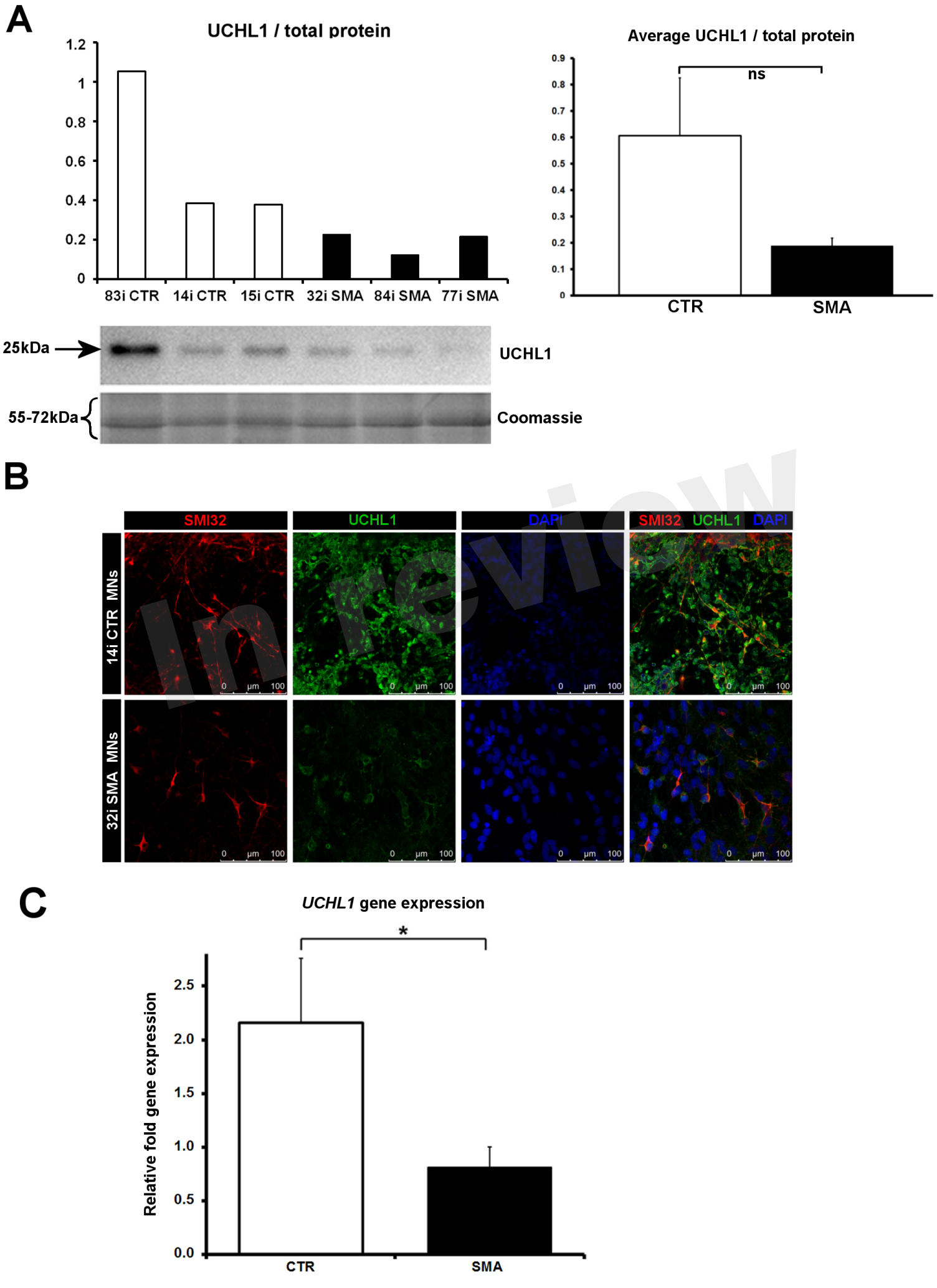
A
UCHL1 / total protein
1.2
1
0.8
0.6
0.4
0.2
0
83i CTR
14i CTR
15i CTR
32i SMA
84i SMA
77i SMA
Average UCHL1 / total protein
ns
0.9
0.8
0.7
0.6
0.5
0.4
0.3
0.2
0.1
0
CTR
SMA
25kDa
UCHL1
55-72kDa
Coomassie
B
SMI32
UCHL1
DAPI
SMI32 UCHL1 DAPI
14i CTR MNs
32i SMA MNs
0 µm 100
C
UCHL1 gene expression
*
Relative fold gene expression
2.5
2.0
1.5
1.0
0.5
0.0
CTR
SMA

Figure 6.TIF